STATISTICAL EVALUATION OF APATITE-LIKE PRECURSOR PREPARATION METHODS FROM THE VIEWPOINT OF POROUS CALCIUM PHOSPHATE CERAMICS

Ľ. Medvecký, M. Kašiarová, H. Bruncková, J. Mihalik

Abstract

The apatite-like powder precursors were synthesized by neutralization and precipitation methods. Ceramic scaffolds with approx. 15 vol.% porosity were prepared by sintering at 1150°C. Mechanical properties, microstructure and phase composition of porous calcium phosphate ceramic samples were studied and compared. Bi- and three-phasic systems were obtained after sintering of samples depending on the starting precursor type. Generally samples prepared from a precipitated precursor had wider values of variances in several studied parameters, despite of the synthesis of apatite-like phase from solutions. Ceramic scaffolds have fully acceptable phase compositions, microstructures and compressive strengths from the viewpoint of their utilization in reconstructive or regenerative medicine.

Keywords: hydroxyapatite, mechanical properties, microstructure

INTRODUCTION

Porous calcium phosphate scaffolds have large utilization in reconstructive and regenerative medicine and application in medical practice are determined by the mechanical, physico-chemical properties and microstructure characteristics such as particle size and pore size distribution. Scaffolds have to serve some functions e.g. the support of the cell migration, proliferation, osteoconduction, the formation and growth of new tissues. It has been found that the wide pore size distribution is the best from the point of view new bone tissue formation. The larger pores around 100-200 μm showed bone ingrowth, smaller - ingrowths of unmineralized osteoid tissue and pores with micrometer dimensions can be penetrated only by the fibrous tissues [1]. It is believed that the microporosity contributes to protein adsorption improving, and more intensive body fluid exchange. Besides, the cell adhesion, proliferation and detachment strength are surface roughness sensitive and are increased as the roughness of hydroxyapatite substrate rise [2].

The most common techniques used to create porosity in a biomaterials are salt leaching, gas foaming, phase separation, freeze-drying. The porosity of hydroxyapatite or calcium phosphate ceramics can be affected by admixing various organic binders (e.g. polyvinyl alcohol, cellulose, dispersants) to the powder precursor [3,4]. Two basic methods are used for the hydroxyapatite preparation – neutralization and precipitation methods, which could be modified by the addition of other substances like, for example, EDTA [5], citric acid [6], polyacrylic acid [7] etc. Some effects such as purity of raw material [8], atmosphere, pH [9], temperature, aging time [10,11] on morphology and crystallinity of hydroxyapatite nanoparticles were evaluated. The study of the influence of powder processing and sintering temperature on densification, microstructure and mechanical

Ľubomír Medvecký, Monika Kašiarová, Helena Bruncková, Ján Mihalik, Institute of Materials Research, Slovak Academy of Sciences, Košice, Slovak Republic

properties of hydroxyapatite ceramics prepared from precipitated hydroxyapatite showed that the maximal densification was achieved at a temperature of 1100°C [12].

The dependence of the compressive strength on the hydroxyapatite ceramic porosity is generally well-described by an exponential behaviour based on the minimum solid area approach. [23]. The results of Heuc et al. [24] indicated that not only the total porosity but also pore size can influence the compressive strength. Gibson and Ashby [25] reported proportional correlation between the apparent density and the mechanical strength.

In this paper, mechanical properties, microstructure and phase composition of porous calcium phosphate ceramic scaffolds prepared from apatite-like precursors are studied and compared. Precursors were synthesized by precipitation and neutralization methods. Apart from the aim of the experimental works was the preparation of ceramic scaffolds with compressive strength around 200 MPa, which corresponds to the strength of compact bone.

EXPERIMENTAL PROCEDURE

Method A

Hydroxyapatite A was synthesized by the slow addition of H_3PO_4 (8.5%, analytical grade) to $Ca(OH)_2$ (Europ. Pharm. grade) water suspension. The calculated Ca/P ratio from reactant stoichiometry was 1.67. The suspension was milled in a polyethylene jar with porcelain balls for 2 hours and aged for 20 hours. The final pH suspension was adjusted to 8.5 by a few drops of orthophosphoric acid, filtered, washed with distilled water and dried at 105°C for 4 hours.

Method B

Hydroxyapatite B was synthesized by the co precipitation of 0.5M $Ca(NO_3)_2 \cdot 4H_2O$ (analytical grade) solution and 0.5M $(NH_4)_2HPO_4$ (analytical grade) solution (molar ratio of Ca/P = 1.66). The aqueous solution of $Ca(NO_3)_2 \cdot 4H_2O$ was slowly dropped into $(NH_4)_2HPO_4$ aqueous solution for 1.5 hour. The pH at the end of the experiments was adjusted and kept at 10.5 by adding NH_3(aq) (1:1). The rotation speed of stirrer was 450 rpm and precipitation was done at 25°C. Ageing time was 72 h. Precipitates were washed with distilled water and filtered over the membrane filter (Millipore, 0.2 _m pore size). Hydroxyapatite powders were dried at 110°C for 4 h.

The dry powders were crushed and sieved (Mesh 250). Powder mixtures were, after drying, pressed at 70 MPa into pellet form (diameter equals 13 mm) and sintered at 1150°C for 1 hour. For statistical purposes, three powder precursors were prepared by each method.

The phase composition of samples was analysed by X-ray diffraction analysis (Philips X_ PertPro) and infrared spectroscopy (SPECORD M80, 400 mg KBr+1 mg sample). The final Ca/P ratio in scaffolds was determined by chemical analysis after their dissolution in HNO_3(1+3), where calcium was determined by complexometry and phosphorus as P-Mo-V complex by colorimetry. Specific surfaces of hydroxyapatites were measured by the BET method (N_2 adsorption at −196°C, GEMINI). Morphology and particle size of apatite-like powder samples were observed by transmission electron microscopy (TEM, TESLA 500). pH values of solutions were adjusted using a pH-meter (WTW, Inolab 720) with the combined electrode SenTix 41. The microstructure of scaffolds was observed using scanning electron microscopy (SEM, (JEOL FE SEM JSM-7000F). The compressive strength of the ceramic samples was measured by a LR5K Plus (Lloyd Instruments, Ltd.) at the loading rate of 0.5 mm min^{-1}. The densities of scaffolds

were calculated from their dimensions and weights. The statistical evaluation of various parameters both precursors and ceramic scaffolds was done using ANOVA analysis at level $\alpha = 0.05$.

RESULTS AND DISCUSSION

In Figure 1, microstructures of fractured calcium phosphate ceramic scaffolds prepared from precursor A and B are shown. The transgranular fracture mode is clearly visible in both microstructures and average grain size was approximately 1 µm. Irregular small pores of micrometer dimension were found in scaffolds. Grains had a characteristic angular shape which corresponds with the hexagonal crystallographic symmetry of hydroxyapatite. No significant differences were observed in microstructures. The relative densities of ceramic samples A (85%) and B (83%) were not statistically different, but the significant statistical difference was found in the case of scaffold B relative densities. Note that standard deviations of relative densities in individual sample group were low. The particles in prepared apatite-like powder precursors were represented by the spherical morphology (Figs.2a,b). The average particle sizes of apatite-like precursors A and B were ~80 nm and ~50 nm. The smaller particle size in precursors B verifies a higher mean value of specific surface equal 96.4 ± 7.9 m^2/g contrary to 73 ± 5.2 m^2/g of precursors A. The particle size distributions are characterized by bimodal curves (Figs.3a,b), where d_{50} values equal 5 and 9 µm for A and B precursors, respectively. From comparison of distribution curves and d_{50} values is seen that the maximum distribution density of particle agglomerates is shifted to higher agglomerate dimension in the case of B precursors. Thus the finer particles in precursor B are arranged to larger agglomerates probably as the result of electrostatic surface attraction forces of individual particles and capillary forces given the water molecules adsorption.
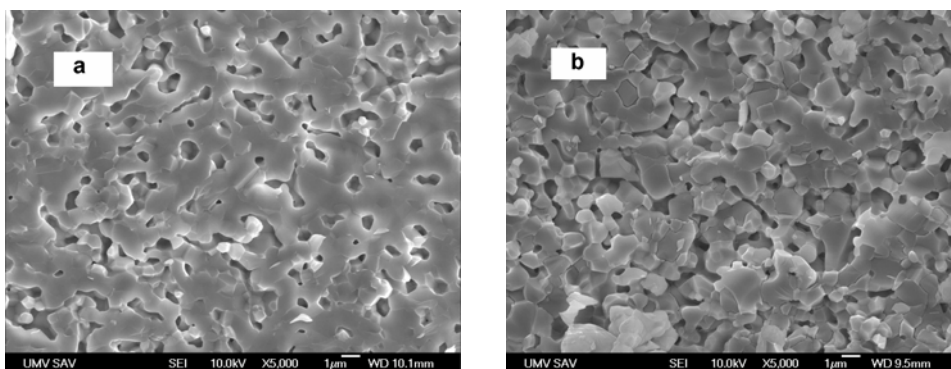

Fig.1. Microstructures of fractured calcium phosphate ceramics prepared from precursor A (a) and B (b).
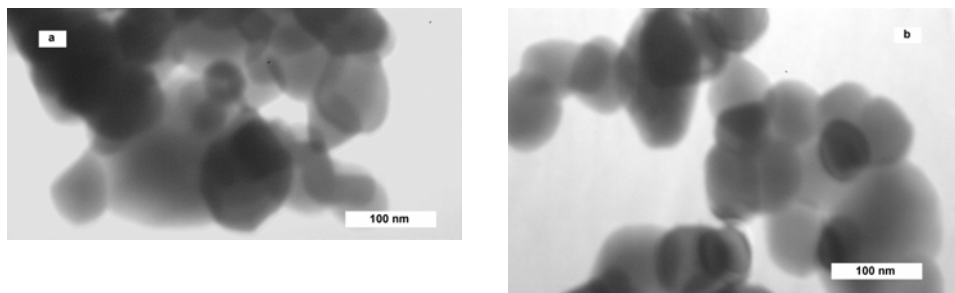
Fig.2. Morphology of apatite-like particles in powder precursors A (a) and B (b).
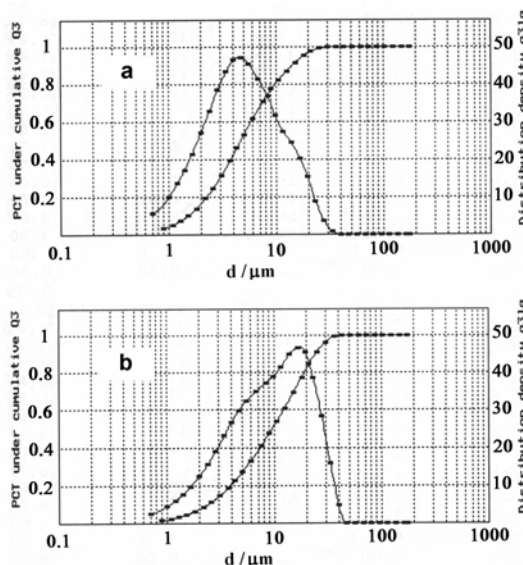

Fig.3. Particle size distribution curves of precursor A (a) and B (b).

XRD diffraction patterns of samples are shown in Figs.4a,b,c. The patterns of powder precursors did not differ one from another and the nanoapatite phase (JCPDS 24-0033) was present in both types of unannealed samples (Fig.4a). Two ultimate phases were found in patterns of ceramics A – β-tricalcium phosphate (βTCP, JCPDS 09-0169) and hydroxyapatite (HAP, JCPDS 24-0033). In XRD patterns of ceramics B, apart from phases observed in ceramics A, the lines from reflections of αTCP phase (JCPDS 29-0359) planes are visible. The crystallinity sizes calculated from reflections of (002) hydroxyapatite plane using the Scherrer equation were 30 nm and 35 nm in ceramics B and A, respectively. The phase compositions of samples were determined by the Rietveld method (Rietica, LHPM program [13]). At the first step 2θ zero point, unit cell constants were refined together with the simulation of the background and peak shape using, respectively, 6th-order polynomial and asymmetric pseudo-Voigt functions. The ceramics A contained 21±11 wt% βTCP. The mean contents of βTCP and αTCP in ceramics B were 17±12 wt% and 14±7 wt% respectively. Thus, the total hydroxyapatite content in ceramics B was minimally 70 wt.% contrary to about 80 wt.% in the case of ceramics A. The precursor B was more sensitive to

the thermal decomposition at 1150°C, where the high temperature phase represented αTCP. The Ca/P ratios in ceramics A and B were 1.72±0.035 and 1.7±0.10, where variance in values B was caused by differences in phosphorus content. A small CaO amount was observed in both patterns only probably as the result of the insufficient crystallinity of fine particles. Regardless of the precursor B precipitation from homogeneous solution environments, the final stoichiometry in ceramic scaffolds did not correspond with starting stoichiometry of pure hydroxyapatite. In the case of scaffolds A, the principally different formation way of reaction product has to be considered, where phosphate ions diffuse via calcium phosphate layer on $Ca(OH)_2$ particle surfaces and the reaction need not take place with 100% efficiency. Note that amounts of main precipitated ions in starting reactants were not analysed before reactions.
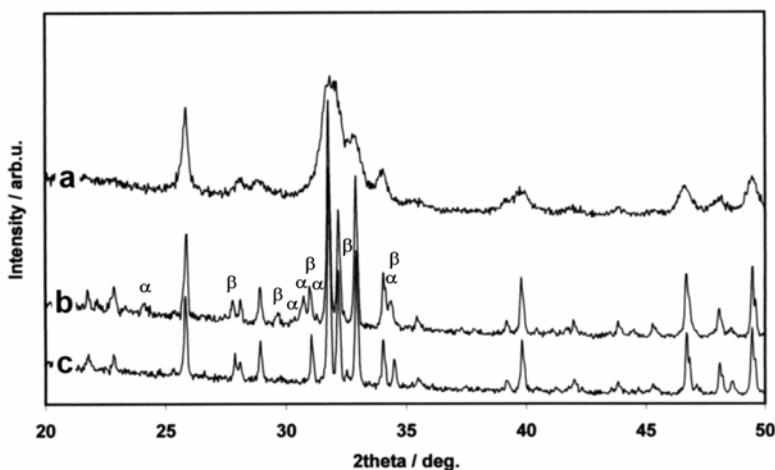

Fig.4. XRD patterns of powder precursor A (a), ceramics B (b) and ceramics A (c).

In IR spectra of both ceramic precursors (Fig.5a,b), the band around 1650 cm^{-1} indicate adsorbed H_2O, the characteristic vibration of the PO_4^{3-} group are located at 1050, 1100 and 962 cm^{-1} (antisymmetric (v_3) and symmetric (v_1) P-O stretching vibrations), O-P-O bending (v_4) vibrations at 565 and 603 cm^{-1}, v_2 and v_3 modes of CO_3^{2-} at wavenumbers of 870 and 1400 - 1550 cm^{-1} and the librational mode at 630 cm^{-1} and the stretching vibration at 3570 cm^{-1} of OH hydroxyapatite group can be found in spectra [6,14]. Peaks correspond to CO_3^{2-} group vibrations at 1420, 1460, 1550 and 870 cm^{-1} representing the carbonated hydroxyapatite types − A-type with CO_3^{2-} substitution for OH groups characterized by a band from CO_3^{2-} vibration at 1550, 1460 cm^{-1} and B-type with CO_3^{2-} substitution for PO_4^{3-} groups with a band at 1460, 1420 cm^{-1}[15,16]. No band at 1550 cm^{-1} was visible in the spectrum of precursor B − this verifies the presence B-type carbonate hydroxyapatite only contrary to precursor A with both types hydroxyapatite. These results clearly indicate that some fraction of phosphate ions was substituted for carbonate ions, and Ca/P ratios have to be shifted to higher values. The average CO_3^{2-} content estimated according to [15] was approximately 4 wt.%. The changes in phosphate band intensities were found in spectra of ceramics which correspond with the tricalcium phosphate formation. Apart from peaks from carbonate vibrations missing from spectra due to carbonate thermal decomposition during sintering.
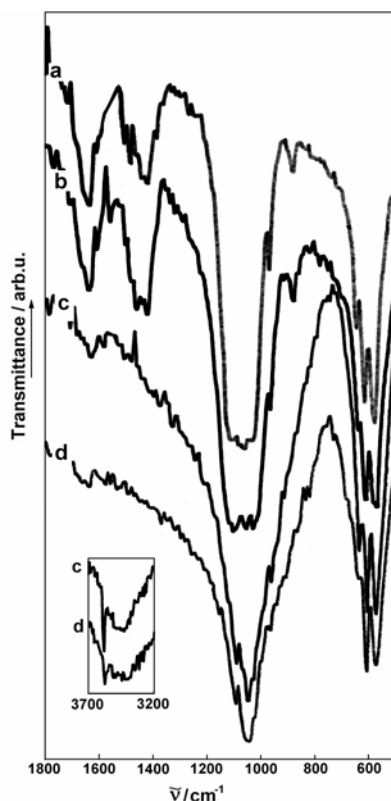
Fig.5. IR spectra of powder precursors A (b), B (a) and ceramics A (d), B (c).

Average compressive strengths (CS) of ceramics A and B were 290±17 MPa and 340±50 MPa. No significant statistical difference was found between these values. On the other hand, larger compressive strength variance was observed in ceramics B and mean CS values of individual samples B were significantly statistically different. Although the large amounts of strength data are reported in literature, the comparison with these is difficult and often impossible due to the different testing procedure and processing methods resulting in the various grain and pore size distribution, phase composition, etc. These and other characteristics significantly influence the final strength of material. It has been reported [26] that the compressive strength of material with similar composition as in our study (73 wt.% of HA and 27 wt.% of βTCP) was 544±54 MPa, and authors also observed a strength value increase with the β-TCP phase amount. The higher values of strength can be simply explained by the lower porosity (3-6%) compared to the porosity of material studied in our work (about 15%). Leibschner [27] summarized the strength of cortical and trabecular bone tissues - human and animal. According to the measured compressive strength values, the studied materials can have potential utilization for the cortical bone implants. Hench and Wilson [28] reported the compressive strength of human cortical bone between 100-230 MPa.

As resulting from the above analysis, generally samples B had wider values of variances in several studied parameters in comparison with samples A, despite the precipitation of apatite-like phase from solutions. Precursor preparation methods make no fully comparable results e.g. in values of specific surfaces or crystallinity, carbonate

substitution or final phase composition of ceramic scaffolds which may influence the behaviour of materials after implantation. It has been found that the β-TCP phase is formed in ceramics prepared by the neutralization method (A) above 900°C, whereas low-crystalline hydroxyapatite, with a comparable specific surface to our precursors A, was prepared [17]. The higher Ca/P ratio (up to 1.7) in precursor A stabilized hydroxyapatite to its thermal decomposition (to β-TCP phase) and another phase – CaO - was only observed above the Ca/P ratio 1.7 [18]. In the case of apatite-like phases prepared by the precipitation method B, similar critical Ca/P ratio was shown and the β-TCP phase volume fraction was minimal at this point. Biphasic calcium phosphate ceramics were prepared from precipitated hydroxyapatite and it contained α- or β-TCP besides the major hydroxyapatite phase above 1000°C [20]. The solubility of biphasic calcium phosphate materials in water solutions increased with the tricalcium phosphate content [6] and αTCP is a more soluble substance than β-TCP [22]. It has been found that the bioresorption strongly affects the bioactivity of calcium phosphate implants and approximately double of the new bone tissue amount was formed in βTCP than in pure hydroxyapatite implants [21]. This fact verifies knowledge that a sequence of events at the surface of bioactive materials promotes bone healing and osteogenesis [22]. Thus, prepared ceramic scaffolds have fully acceptable phase compositions, microstructures and compressive strengths from the viewpoint of their utilization in reconstructive or regenerative medicine.

CONCLUSIONS

Two calcium phosphate precursors were synthesized by neutralization and precipitation methods, and following, were utilized for the preparation of ceramic scaffolds. The final nanoapatite-like powders have large specific surfaces and contained around 4 wt.% carbonates. Bi- and three- phasic systems were obtained after sintering materials at 1150°C, where hydroxyapatite, βTCP phases were found in ceramics prepared from precursor A and the additional αTCP phase was created in the case of ceramics prepared from precursor B. The porosities of ceramic scaffolds were around 15 vol.%. The compressive strengths of ceramics A and B were 290 and 340 MPa. Precursor preparation methods make no fully comparable results, e.g. in values of specific surfaces or crystallinity, carbonate substitution or final phase composition of ceramic scaffolds, which may influence the behaviour of materials after implantation.

Acknowledgement

REFERENCES

[1] Karageorgiou, V., Kaplan, D.: Biomaterials, vol. 26, 2005, p. 5474
[2] Deligianni, DD., Katsala, ND., Koutsoukos, PG., Missirlis, YF.: Biomaterials, vol. 22, 2001, p. 87
[3] Landi, E., Tampieri, A., Celotti, G., Langenati, R., Sandri, M., Sprio, S.: Biomaterials, vol. 26, 2005, p. 2835
[4] Deville, S., Saiz, E., Tomsia, AP.: Biomaterials, vol. 27, 2006, p. 5480
[5] Bezzi, G., Celotti, G., Landi, E., La Torretta, TMG., Sopyan, I., Tampieri, A.: Materials Chemistry and Physics, vol. 78, 2003, p. 816
[6] Pena, J., Vallet-Regi, M.: Journal of the European Ceramic Society, vol. 23, 2003, p.

1687

[7]　Sz-Chian Liou, San-Yuan Chen, Dean-Mo Liu: Biomaterials, vol. 24, 2003, p. 3981

[8]　Bernard, L., Freche, M., Lacout, JL., Biscant, B.: Powder Technol., vol. 103, 1999, p. 19

[9]　Afshar, A., Ghorbani, M., Ehsani, N., Saeri, MR., Sorrell, CC.: Mater.Design., vol. 24, 2003, p. 197

[10]　Smiciklas, I., Onjia, A., Raicevic, S.: Sep. Purif. Technol., vol. 44, 2005, no. 2, p. 97

[11]　Pang, YX., Bao, X.: J. Europ. Ceram. Soc., vol. 23, 2003, p. 1697

[12]　Thangamani, N., Chinnakali, K., Gnanam, FD.: Ceramics International, vol. 28, 2002, p. 355

[13]　Hunter, BA., Howard, CJ.: LHPM—A Computer Program for Rietveld Analysis of X-ray and Neutron Powder Diffraction Patterns. Lucas Heights, Research Laboratories, Australia, 2000

[14]　Panda, RN., Hsieh, MF., Chung, RJ., Chin, TS.: Journal of Physics and Chemistry of Solids, vol. 64, 2003, p. 193

[15]　Krajewski, A., Mazzocchi, M., Buldini, PL., Ravaglioli, A., Ravaglioli, A., Tinti, A., Taddei, P., Fagnano, C.: J. Molecular Struc., vol. 744-747, 2005, p. 221

[16]　Apfelbaum, F., Diab, H., Mayer, I., Featherstone, JDB.: J. Inorg.Biochem., vol. 45, 1992, p. 277

[17]　Lazic, S., Zec, S., Miljevic, N., Milonjic, S.: Termochimica Acta, vol. 374, 2001, p. 13

[18]　Osaka, A., Miura, Y., Takeuchi, K., Asada, M., Takahashi, K.: J. Mater. Sci.:Mater. Med., vol. 2, 1991, p. 51

[19]　Sung, YM., Lee, JC., Yang, JW.: J. Crystal Growth, vol. 262, 2004, p. 467

[20]　Petrov, OE., Dyulgerova, E., Petrov, L., Popova, R.: Mater. Lett., vol. 48, 2001, p. 162

[21]　Kanamura, S., Sasano, Y., Shimizu, T., Hatori, K., Suzuki, O., Kagayama, M., Motegi, K.: J. Biomed. Mater. Res., vol. 59, 2002, p. 29

[22]　LeGeros, R.: Clinical Mater., vol. 14, 1993, p. 65

[23]　Rice, RW.: J. Mater. Sci.,vol. 28, 1993, p. 2187

[24]　Le Huec, JC., Schaeverbeke, T., Clement, D., Faber, J., Le Rebeller, A.: Biomaterials, vol. 16, 1995, p. 113

[25]　Gibson, LJ., Ashby, MF.: Cellular Solids: Structure and Properties, Cambridge Solid State Science Series. 2nd ed. Cambridge University Press, 1997

[26]　Zyman, ZZ., Tkachenko, MV., Polevodin, DV.: J. Mater. Sci: Mater. Med., vol. 19, 2008, p. 2819

[27]　Liebschner, MAK.: Biomaterials, vol. 25, 2004, p. 1697

[28]　Hench, LL., Wilson, J.: An Introduction to Bioceramics. London : World Scientific, 1993